


 Cite this: *RSC Adv.*, 2022, **12**, 22826

## Mutations responsible for the carbapenemase activity of SME-1<sup>†</sup>

 Vidhu Agarwal, Akhilesh Tiwari and Pritish Varadwaj \*

SME-1 is a carbapenemase, produced by *Serratia marcescens* organism and causes nosocomial infections such as in bloodstream, wounds, urinary tract, or respiratory tract infections. Treatment of such infections becomes very complex due to its resistance towards penicillins, cephalosporins, monobactams, and carbapenems. Resistance to such antibiotics is of great medical concern. The misuse and overuse of these antibiotics result in the clinical mutation and production of novel  $\beta$ -lactamase enzymes such as SME-1, which show resistance to carbapenems. Class A contains most of the clinically significant extended spectrum of  $\beta$ -lactamase enzymes and carbapenemases. In this study, class A  $\beta$ -lactamase SME-1 sequence, structure, and binding were compared with naturally mutated class A  $\beta$ -lactamase enzymes and a wild-type TEM-1. This study was performed for revealing mutations, which could be responsible for the carbapenemase activity of SME-1. The dynamic characteristics of SME-1 enzymes manifest a different degree of conservation and variability, which confers them to possess carbapenemase activities. Met69Cys, Glu104Tyr, Tyr105His, Ala237Ser, and Gly238Cys mutations occur in SME-1 as compared to wild-type TEM-1. These mutated residues are present close to active site residues such as Ser70, Lys73, Ser130, Asn132, Glu166, and Asn170, which participate in the hydrolytic reaction of  $\beta$ -lactam antibiotics. Furthermore, these mutated residues demonstrate altered interactions with the  $\beta$ -lactam antibiotics (results in altered binding) and within themselves (results in active site structure alterations), which results in expanding the spectrum of activity of these enzymes. This study provides important insights into the structure and activity relationship of SME-1 enzymes. This is evident from the  $\Omega$ -loop structure modification, which forms the wall of the active site and repositioning of residues involved in hydrolytic reactions, when present in the complex with meropenem in a stable state of MD simulation at 50 ns. Hence, Met69Cys, Glu104Tyr, Tyr105His, Ala237Ser, and Gly238Cys mutations could result in an altered active site structure, binding, and activity of SME-1 with meropenem and thus become resistant against meropenem, which is a carbapenem.

Received 5th May 2022  
 Accepted 12th July 2022

DOI: 10.1039/d2ra02849b  
[rsc.li/rsc-advances](http://rsc.li/rsc-advances)

### Introduction

Carbapenems are broad-spectrum antibiotics, with enhanced stability against hydrolysis. The loss of the outer membrane permeability and the development of  $\beta$ -lactam hydrolyzing enzymes have been identified as one of the key mechanisms of carbapenem resistance. This results in one of the most resilient  $\beta$ -lactamase enzymes termed carbapenemase.<sup>1</sup> *Serratia marcescens* enzyme (SME) was identified as a class A carbapenemase, which was derived from two clinical strains of *Serratia marcescens* (in 1982) from England, Europe, North America, and South America. SME carbapenemase being atypical in nature, manifest a distinctive phenotypic profile, exhibiting tolerance to all  $\beta$ -lactams except extended-spectrum cephalosporins

(ceftazidime and cefepime), including carbapenems and aztreonam.<sup>2</sup> *Serratia marcescens* causes community-acquired and nosocomial infections such as the circulation, wounds, urinary system, and respiratory tract. With the emergence of resistance, it has become extremely challenging to curb this pathogenic organism.<sup>3,4</sup> The basic architecture and folds of the SME-1 structure are considerably comparable to those of class A beta-lactamase enzymes. Almost all the key active site residues positioned in SME-1 are conserved among class A  $\beta$ -lactamases except at 104, 105, and 237 loci, which are occupied by tyrosine, histidine, and serine, respectively.<sup>5</sup> Cysteine at loci 238 forms a disulfide bridge with another cysteine positioned at 69 loci. The critical function of this disulfide bridge was substantiated by the site-directed substitution of Cys69 to Ala that produced an incapable variant that fails to impart resistance to imipenem and all other assayed  $\beta$ -lactams. The noteworthy structural characteristic of SME-1 was the positioning of the active site serine (70) residue and glutamate (166) by a minuscule distance of up to 1.4 nm compared to class A  $\beta$ -lactamases. As a result,

Indian Institute of Information Technology, Devghat, Jhalwa, Prayagraj-211015, Allahabad, U P, India. E-mail: [pritish@iiti.ac.in](mailto:pritish@iiti.ac.in); Tel: +919236666060

<sup>†</sup> Electronic supplementary information (ESI) available. See <https://doi.org/10.1039/d2ra02849b>

the three-dimensional active site topology of SME-1 fails to accommodate the vital catalytic  $\text{H}_2\text{O}$  molecules located between Ser70 characterized in class A beta-lactamases. This entails a significant conformational alteration in SME-1, which may be required for the appropriate positioning of the hydrolytic water molecule and directly implicated in the hydrolysis of the acyl-enzyme intermediate.<sup>6</sup>

The SME-1 carbapenemase Ser237Ala mutant displayed penicillin and aztreonam hydrolysis almost similar to wild-type class A  $\beta$ -lactamase enzyme but showed reduced susceptibility against cefoxitin, cephaloridine, and cephalothin. A sharp decline in the catalytic efficiency was observed against the imipenem, signifying the pertinent role of a serine residue in SME-1 carbapenemase activity.<sup>6</sup> The significance of the disulfide linkage across Cys69 and Cys238 in the carbapenem hydrolysis, as well as other  $\beta$ -lactams, was also demonstrated. The loss of catalytic activity by the SME-1 carbapenemase Cys69Ala mutant against imipenem, cefoxitin, kanamycin, ticarcillin, amoxicillin, and aztreonam has been observed.<sup>5</sup> PCR-based mutations have been used to generate different alternative libraries for both the Cys69 and Cys238 positions. Those enzymes from either of these libraries having Cys69 and Cys238 showed efficiency and competence in conferring resistance to  $\beta$ -lactams, indicating how these cysteines and the associated disulfide linkage are unfavorable to the hydrolysis of all  $\beta$ -lactam degraded by SME-1.<sup>7</sup> Furthermore, SME-1 residues at 104, 105, 132, 167, 237, and 241 were subjected to randomised site-directed mutations, and proficient mutants were identified based on their capacity to hydrolyze imipenem, ampicillin, and cefotaxime. However, no specific site appeared essential for carbapenem hydrolysis, numerous locations appeared to be significant for  $\beta$ -lactam antibiotic hydrolysis, indicating that the carbapenemase activity of SME-1 is the consequence of a highly dispersed series of interactions that gradually modulates the conformation and architecture of the active site compartment.<sup>8</sup>

Functional insights into drug resistance can be found using MD simulation methods. Further, an atomic level of understanding can be gained using post-simulation methods such as PCA. This method enables the dimensionality reduction of different parameters of MD simulation in order to have an understanding of its concerted motion.<sup>9</sup> PCA analysis can help in knowing the effect of mutation on the overall MD trajectory; hence, it is also known as essential dynamics.<sup>10</sup> RIN and residual decomposition analysis help in knowing the effect of mutation on the protein residue interaction network and free energy change at the residue level, respectively.

This study focuses on determining the mutations responsible for the carbapenemase activity of SME-1 class A  $\beta$ -lactamase enzymes. This could be known from the comparison of sequence, structure, and interactions of SME-1 with naturally mutated and wild-type class A  $\beta$ -lactamase enzymes, in complex with  $\beta$ -lactam antibiotics. Further, molecular docking, MMGBSA, RMSD, and PCA analysis help in getting insights into the stability of SME-1 carbapenemase, as compared to naturally mutated and wild-type TEM-1 class A  $\beta$ -lactamase enzymes in complex with  $\beta$ -lactam antibiotics.

## Results

SME-1 has evolved clinically to extend its spectrum against the most effective and last resort of  $\beta$ -lactam antibiotics like carbapenems. Usually, the structures of these enzymes are conserved, including their active site residues such as Ser70, Lys73, Ser130, Asn132, Glu166, and Asn170 (for class A  $\beta$ -lactamase enzymes), which participate in the hydrolytic reaction with  $\beta$ -lactam antibiotics. The mutation of some important residues could alter the structure and activity of such  $\beta$ -lactamase enzymes.<sup>11</sup> This could be due to alterations in the interaction pattern of the  $\beta$ -lactamase enzymes within themselves (active site structure alterations) and with  $\beta$ -lactam antibiotics (binding alteration), which could result in structural and functional modifications. These structural modifications caused due to mutations result in alterations in binding with the ligand and hence could be responsible for the carbapenemase activity of SME-1. Kinetic, molecular docking, molecular dynamic simulation, PCA, and MMGBSA analysis revealed altered interactions and stability of the SME-1 in complex with amoxicillin, ceftazidime, ceftolozane, and meropenem as compared to wild-type TEM-1 and naturally mutated class A  $\beta$ -lactamase enzymes.

### Kinetics analysis

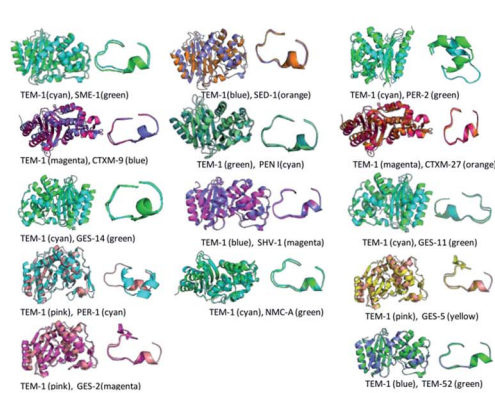
Naturally mutated SME-1 class A  $\beta$ -lactamase is a carbapenemase.<sup>12</sup> The catalytic efficiency of wild TEM-1 class A  $\beta$ -lactamase is  $0.002 \mu\text{M}^{-1} \text{s}^{-1}$  as compared to the catalytic efficiency of clinically mutated SME-1 that is  $0.44 \mu\text{M}^{-1} \text{s}^{-1}$  in complex with imipenem. Similarly, Table S1† shows the difference in catalytic efficiency of clinically mutated class A  $\beta$ -lactamase enzymes (SME-1 and SHV-1) and wild TEM-1 enzyme with respect to different  $\beta$ -lactam antibiotics. Further, from Table S1,† it is evident that the catalytic efficiency ( $K_{\text{cat}}/k_{\text{m}}$ ) of SME-1 is higher, as compared to that of GES-1, GES-11, and GES-5, TEM-1 for cephalothin, cefoxitin and imipenem (carbapenem).

### Sequence analysis

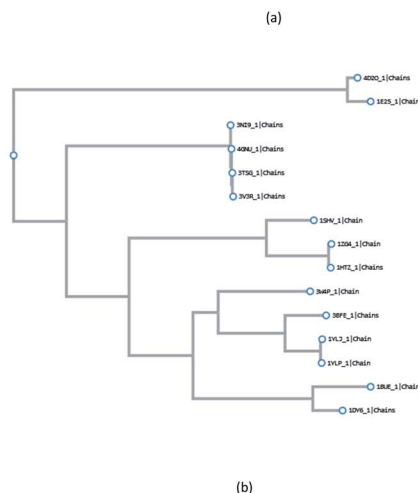
14 naturally mutated and wild-type class A  $\beta$ -lactamase enzyme sequences were compared. Multiple sequence alignment results are shown in Fig. 1a. Furthermore, Table 1 combines the residues that could be indirectly involved in the alteration of  $\beta$ -lactam activity and the mutations present in 14 naturally mutated and wild-type class A  $\beta$ -lactamase enzyme sequences. Fig. 1b shows that TEM-1 (PDB ID: 1ZG4) and SHV-1 (PDB ID: 1SHV) are evolutionary very close. Further, SME-1 (PDB ID: 1DY6) is evolutionary very far from TEM-1 and SHV-1. As SHV-1 is a penicillinase (Table 1), it has a similar binding affinity with the TEM-1 enzyme and has a similar  $\Omega$ -loop structure (Fig. 1c) and a lesser number of mutations on residues that could be indirectly involved in the alteration of the  $\beta$ -lactam activity, as compared to TEM-1 (Table 1). Therefore, for further analysis and comparison, the SHV-1 enzyme is selected as a naturally mutated class A  $\beta$ -lactamase enzyme, which can be compared with naturally mutated class A  $\beta$ -lactamase enzyme SME-1 with carbapenemase activity.



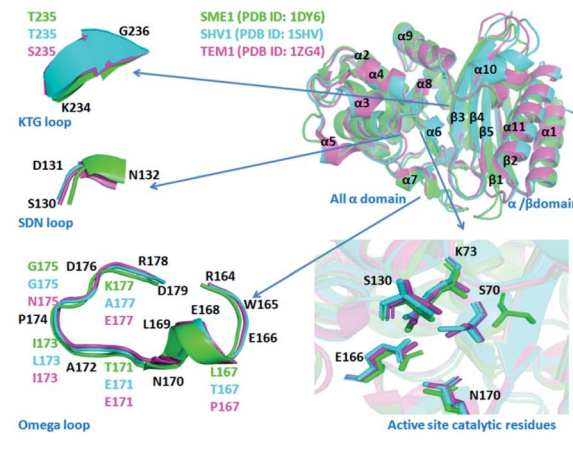
1254\_11Chains 10 20 30 40 50 60 70 80 90 100 110 120  
 1012\_11Chains 10 20 30 40 50 60 70 80 90 100 110 120  
 1587\_11Chains 10 20 30 40 50 60 70 80 90 100 110 120  
 1093\_11Chains 10 20 30 40 50 60 70 80 90 100 110 120  
 1086\_11Chains 10 20 30 40 50 60 70 80 90 100 110 120  
 3081\_11Chains 10 20 30 40 50 60 70 80 90 100 110 120  
 1132\_11Chains 10 20 30 40 50 60 70 80 90 100 110 120  
 1115\_11Chains 10 20 30 40 50 60 70 80 90 100 110 120  
 3049\_11Chains 10 20 30 40 50 60 70 80 90 100 110 120  
 4020\_11Chains 10 20 30 40 50 60 70 80 90 100 110 120  
 Consensus 10 20 30 40 50 60 70 80 90 100 110 120  
  
 1254\_11Chains 140 150 160 170 180 190 200 210 220 230 240 250  
 1012\_11Chains 140 150 160 170 180 190 200 210 220 230 240 250  
 1587\_11Chains 140 150 160 170 180 190 200 210 220 230 240 250  
 1093\_11Chains 140 150 160 170 180 190 200 210 220 230 240 250  
 1086\_11Chains 140 150 160 170 180 190 200 210 220 230 240 250  
 3081\_11Chains 140 150 160 170 180 190 200 210 220 230 240 250  
 1132\_11Chains 140 150 160 170 180 190 200 210 220 230 240 250  
 1115\_11Chains 140 150 160 170 180 190 200 210 220 230 240 250  
 3049\_11Chains 140 150 160 170 180 190 200 210 220 230 240 250  
 4020\_11Chains 140 150 160 170 180 190 200 210 220 230 240 250  
 Consensus 140 150 160 170 180 190 200 210 220 230 240 250



(c)



(b)



(d)

**Fig. 1** (a) Multiple sequence alignments of SME-1 (PDB ID: 1DY6) along with 13 naturally mutated class A  $\beta$ -lactamase enzymes (TEM-52 (PDB ID: 1HTZ), SHV-1 (PDB ID: 1SHV), SME-1 (PDB ID: 1DY6), NMC-A (PDB ID: 1BUE), SED-1 (PDB ID: 3BFE), CTXM-9 (PDB ID: 1YLJ), CTXM-27 (PDB ID: 1YLP), PENI (PDB ID: 3W4P), GES-2 (PDB ID: 3NI9), GES-11 (PDB ID: 3V3R), GES5 (PDB ID: 4GNU), PER-1 (PDB ID: 1E25) and PER-2 (PDB ID: 4D2O)) and TEM-1 (PDB ID: 1ZG4). (b) Shows the phylogenetic tree for the (PDB ID: 1DY6) along with 13 naturally mutated class A  $\beta$ -lactamase enzymes and TEM-1 (PDB ID: 1ZG4). (c) Shows overall and  $\Omega$ -loop structure comparison of 14 naturally mutated class A  $\beta$ -lactamase enzymes (including SME-1) with wild type class A  $\beta$ -lactamase enzyme TEM-1. (d) Shows the comparison of SME-1 (carbapenemase), SHV-1 (penicillinase) and TEM-1 (wild type) class A  $\beta$ -lactamase enzyme.

It can be observed from Table 1 that Glu104Tyr has a unique mutation in SME-1, as compared to other naturally mutated class A  $\beta$ -lactamase enzymes with respect to wild-type class A  $\beta$ -lactamase enzyme TEM-1. Tyr105His has a unique mutation, except for NMC-A compared to other clinically mutated class A  $\beta$ -lactamase enzymes with respect to wild-type class A  $\beta$ -lactamase enzyme TEM-1.

### Structure analysis

SME-1 is a carbapenemase. 14 naturally mutated and wild-type class A  $\beta$ -lactamase enzyme structures were aligned and visualized in PyMOL, as shown in Fig. 1c. Further, root mean square deviation (RMSD) calculations were also performed in PyMOL. It was performed on all 14 enzymes as compared to wild-type TEM-1 enzyme.

Class A  $\beta$ -lactamases contain two domains, between which the active site of the enzyme is present. The first domain contains eight  $\alpha$  helix ( $\alpha_2$ - $\alpha_9$ ), whereas the second domain contains five  $\beta$ -strands ( $\beta_1$ - $\beta_5$ ) and three  $\alpha$  helix ( $\alpha_1$ ,  $\alpha_{10}$ ,  $\alpha_{11}$ ). Ser70, Lys73, Ser130, Asn132, Glu166, and Asn170 are conserved in all the naturally mutated class A  $\beta$ -lactamase enzymes and the wild-type class A  $\beta$ -lactamase enzyme. These residues participate in the hydrolytic reaction with  $\beta$ -lactam antibiotics including Ser70, which acts as a nucleophile and attacks the  $\beta$ -lactam ring for its hydrolysis.<sup>13</sup> Ser70 was observed to be displaced in SME-1 by an RMSD value of 0.071, as compared to TEM-1. Ser70 residue in SME-1 is much more structurally recolated as compared to the wild TEM-1 and other clinically mutated class A  $\beta$ -lactamase enzymes. This is caused due to alterations in the active site structure of SME-1, due to clinical mutations as compared to wild TEM-1. It can be observed from Table 2 that Ser70 (0.071) and  $\Omega$ -loop



**Table 1** Shows organism name, activity, PDB ID and mutations occurring in SME1 along with 13 clinically mutated and wild type class A  $\beta$ -lactamase enzymes and the colour highlights depicts  $\Omega$ -loop structure modification: more difference (green), less difference (blue) and without difference (black) as compared to wild type TEM-1. Further, clinically mutated class A  $\beta$ -lactamase enzymes (SME-1 and SHV-1) and wild type class A  $\beta$ -lactamase enzyme (TEM-1) have been highlighted with bold

Organism name	Activity	PDB ID	Protein name	69	104	105	132	164	165	170	171	173	176	178	179	182	216	237	238	240	244	271	273	274
<i>Escherichia coli</i>	Wild type	1ZG4	TEM-1	Met	Glu	Tyr	Asn	Arg	Trp	Asn	Glu	Ile	Asp	Asn	Asp	Met	Val	Ala	Gly	Glu	Arg	Thr	Asp	Glu
<i>Klebsiella pneumoniae</i>	Cephalosporinase	1HTZ	TEM-52	Lys																				
<b><i>Klebsiella pneumoniae</i></b>	<b>Penicillinase</b>	<b>1SHV</b>	<b>SHV-1</b>	<b>Asp</b>	<b>Cys</b>	<b>Tyr</b>	<b>His</b>																	
<b><i>Serratia marcescens</i></b>	<b>Carbapenemase</b>	<b>1DY6</b>	<b>SME-1</b>																					
<i>Enterobacter cloacae</i>	Carbapenemase	1BUE	NMC-A	Cys	Phe	His																		
<i>Citrobacter sedlaki</i>	Cephalosporinase	3BFE	SED-1	Cys	Asn	Trp																		
<i>Escherichia coli</i>	Cephalosporinase	1YLJ	CTXM-9	Cys	Asn																			
<i>Escherichia coli</i>	Cephalosporinase	1YLP	CTXM-27	Cys	Asn																			
<i>Burkholderia pseudomallei</i>	Carbapenemase	3W4P	PENI	Cys	Arg																			
<i>Pseudomonas aeruginosa</i>	Carbapenemase	3N19	GES-2	Cys		Trp																		
<i>Acinetobacter baumannii</i>	Carbapenemase	3TSG	GES-14	Cys		Trp																		
<i>Acinetobacter baumannii</i>	Carbapenemase	3V3R	GES-11	Cys		Trp																		
<i>Pseudomonas aeruginosa</i>	Carbapenemase	4GNU	GES-5	Cys		Trp																		
<i>Pseudomonas aeruginosa</i>	Cephalosporinase	1E25	PER-1	Gln	Thr	Trp																		
<i>Citrobacter freundii</i>	Cephalosporinase	4D2O	PER-2	Gln	Thr	Trp																		

loop (0.366) deviation in SME-1 is greater with respect to wild class A  $\beta$ -lactamase enzyme TEM-1, as compared to other clinically mutated class A  $\beta$ -lactamase enzymes like NMC-A, PENI, GES-2, GES-5, GES-11 and GES-14. Further, Fig. 1d shows the structural relocation of Ser70 in SME-1, as compared to SHV-1 and TEM-1.

$\Omega$ -loop and SDN loop forms the wall of the active site and is the most flexible element. Any structural modification in the active site can be easily reflected by the  $\Omega$ -loop structure modification. 6 Carbapenemases NMC-A (0.316), PENI (0.272), GES-2 (0.287), GES-5 (0.274), GES-11 (0.333) and GES-14 (0.273) have a lower RMSD deviation in the  $\Omega$ -loop structure, as compared to the  $\Omega$ -loop structure of naturally mutated SME-1 (0.366) with respect to wild type TEM-1. Among the carbapenemases, SME-1 has the greatest deviation in the  $\Omega$ -loop and SDN loop structure, as compared to wild-type TEM-1. This can be observed from the data in Fig. 1c and d, and Table 2.

### Molecular docking and MMGBSA

The MMGBSA dG bind value gives insights into the binding affinity between the protein and ligand in the docked complex. It is evident from Table 3 that SME-1 has minimum binding energy (MMGBSA dG bind:  $-41.361$  kcal mol $^{-1}$ ) and hence maximum binding affinity for meropenem (carbapenem), as compared to the other 13 naturally mutated class A  $\beta$ -lactamase enzymes and wild-type class A  $\beta$ -lactamase enzymes. Alterations in the binding and affinity of 14 naturally mutated class A  $\beta$ -lactamase enzymes including SME-1 carbapenemase and TEM-1 wild-type class A  $\beta$ -lactamase in the complex with different  $\beta$ -lactam antibiotics evident from the data in Table 3. SME-1 is a carbapenemase and hence has a greater binding affinity ( $-41.361$  kcal mol $^{-1}$ ), as compared to TEM-1 ( $-32.69$  kcal mol $^{-1}$ ) in the complex with meropenem. Further, SME-1 binding affinity is greater depicted by MMGBSA dG bind values ( $-34.84$ ,  $-37.85$ , and  $-62.68$  kcal mol $^{-1}$ ), as compared to TEM-1 ( $-34.53$ ,  $-33.78$ , and  $-15.72$  kcal mol $^{-1}$ ) in complex with amoxicillin, ceftazidime, and cefotolozane as well. This shows that SME-1 is truly a carbapenemase, as it has a greater binding affinity for amoxicillin, ceftazidime, cefotolozane, and meropenem, as compared with TEM-1. Other carbapenemases do not follow a similar binding pattern with amoxicillin, ceftazidime, cefotolozane, and meropenem, except GES-5. GES-5 is a carbapenemase (Table 1) and hence it has a greater binding affinity with amoxicillin ( $-42.59$  kcal mol $^{-1}$ ), ceftazidime ( $-56.46$  kcal mol $^{-1}$ ), and cefotolozane ( $-37.45$  kcal mol $^{-1}$ ), as compared to TEM-1 (Table 3).

SED1 is a cephalosporinase (Table 1) and hence its binding affinity is greater as depicted by MMGBSA dG binding values ( $-36.32$ ,  $-57.02$ , and  $-46.9$  kcal mol $^{-1}$ ), as compared to TEM-1 ( $-34.53$ ,  $-33.78$ , and  $-15.72$  kcal mol $^{-1}$ ) in complex with amoxicillin, ceftazidime, and cefotolozane, respectively. However, in SED-1, the binding affinity is lower ( $-23.305$ ), as compared to TEM-1 ( $-32.69$  kcal mol $^{-1}$ ) in the complex with meropenem. Similar is the case of CTXM-9, CTXM-27, and to some extent NMC-A and PER2, but not with PER1, which all are cephalosporinase class A  $\beta$ -lactamase enzymes (Table 3).

**Table 2** The RMSD values for catalytically important residues, which directly participate in the catalytic hydrolysis of the  $\beta$ -lactam antibiotics and loops present in the active site of clinically mutated class A  $\beta$ -lactamase enzymes, as compared to the TEM-1 wild-type class A  $\beta$ -lactamase enzyme

S. No	Class A $\beta$ -lactamase	$\Omega$ -loop	SDN-loop	Ser70	Lys73	Ser130	Glu166
1	SME1	0.366	0.154	0.071	0.164	0.156	0.051
2	PER2	2.010	0.164	0.045	0.636	0.193	0.058
3	TEM52	0.222	0.094	0.110	0.071	0.049	0.094
4	PENI	0.272	0.126	0.011	0.061	0.264	0.021
5	GES14	0.273	0.195	0.061	0.633	0.217	0.019
6	CTXM9	0.278	0.169	0.094	0.056	0.262	0.024
7	CTXM27	0.241	0.134	0.091	0.119	0.217	0.021
8	GES5	0.274	0.185	0.044	0.117	0.219	0.021
9	PER1	2.029	0.194	0.050	0.089	0.236	0.125
10	SED1	0.372	0.170	0.286	0.173	0.517	0.063
11	GES11	0.333	0.225	0.047	0.632	0.275	0.0402
12	NMCA	0.316	0.178	0.067	0.148	0.027	0.022
13	GES2	0.287	0.236	0.034	0.137	0.203	0.026
14	SHV1	0.212	0.081	0.031	0.041	0.025	0.014

The molecular interactions between the active sites of class A  $\beta$ -lactamase enzymes (SME-1, SHV-1, and TEM-1) and  $\beta$ -lactam antibiotics (amoxicillin, ceftazidime, ceftolozane, and meropenem) were analyzed. In SME-1, Tyr104 does not form any hydrogen bond but is involved in a hydrophobic interaction with ceftazidime and meropenem (Fig. 2a and d). Asp104 of SHV-1 and Glu104 of TEM-1 form a hydrogen bond with amoxicillin, ceftazidime, and meropenem (Fig. 2e and f, Fig. 2h and i, Fig. 2j and l, respectively). This shows that Glu104Tyr mutation in SME-1 plays an important role in altering its binding with amoxicillin, ceftazidime, and meropenem. In SME-1, His105 is involved in polar interaction with amoxicillin, ceftazidime, and meropenem (Fig. 2a and b, and Fig. 2d), respectively. However, in TEM-1 and SHV-1, Tyr105 forms hydrophobic interactions with amoxicillin, ceftazidime, ceftolozane, and meropenem (Fig. 2e–l). This shows that the Tyr105His mutation in SME-1 alters the interaction with amoxicillin, ceftazidime, and meropenem. Glu171 forms an ionic bond with Arg164 and Arg178, which results in an inward turn in the  $\Omega$ -loop.<sup>13</sup> SME-1 contains Glu171Thr mutation (compared to TEM-1), resulting in the disruption of this ionic bond between Arg164, Arg178, and Glu171. The Glu171Thr mutation in SME-1 has a role in altering binding with meropenem (Fig. 2d and l). Thr216 forms a polar interaction in SME-1, whereas Val216 forms hydrophobic interaction in TEM-1, with ceftazidime and meropenem (Fig. 2b, d, j and l). Hence, Val216Thr forms altered interactions in the case of SME-1 with ceftazidime and meropenem, as compared to TEM-1. Two hydrogen bonds are formed between the Ser237 residue of SME-1 and amoxicillin, ceftazidime, and meropenem (Fig. 2a, b and d, respectively). In contrast, no hydrogen bond formation was observed between the Ala237 residue of TEM-1 and SHV-1 with amoxicillin, ceftazidime, and meropenem (Fig. 2e, f, h–j, and l). Hence, Ala237Ser mutation could be responsible for altered interactions between SME-1 and amoxicillin, ceftazidime, and meropenem, as compared to the interaction between wild type TEM-1 and amoxicillin, ceftazidime, and meropenem. One hydrogen bond is formed between the Cys238 residue of SME-1

and meropenem (Fig. 2d), whereas no hydrogen bond is formed between the Gly238 residues of TEM-1 and SHV-1 with meropenem (Fig. 2h and l). Hence, Gly237Cys mutation could be responsible for altered interactions of SME-1 with meropenem, as compared to the interaction between wild type TEM-1 and amoxicillin, ceftazidime, and meropenem. In SME-1, no hydrogen bond is formed between Ala240 and amoxicillin, ceftazidime, ceftolozane, and meropenem (Fig. 2a–d), but in TEM-1, Glu240 forms a salt bridge with ceftazidime (Fig. 2j), four hydrogen bond with ceftolozane (Fig. 2k) and one hydrogen bond with meropenem (Fig. 2l). Hence, Glu240Ala mutation alters interaction in SME-1 with ceftazidime, ceftolozane, and meropenem, as compared with TEM-1.

### Molecular dynamic simulation

**Root mean square deviation (RMSD) analysis.** The RMSD calculations can give an insight into the structural conformation change, throughout the simulation time. The global RMSD of the backbone atom was below 2.5  $\text{\AA}$  for 100 ns, showing the overall stability and absence of significant conformational change in all the cases. The mean RMSD value of SME-1 (1.110) is less, compared with SHV-1 (1.532) and TEM-1 (1.283) with meropenem. The values are tabulated in Table S2.<sup>†</sup> Furthermore, Fig. 3 and the above values suggest that the naturally mutated class A  $\beta$ -lactamase enzyme SME-1 has a better binding with meropenem and amoxicillin, as compared to SHV-1 and TEM-1.

**Root mean square fluctuation (RMSF) analysis.** The RMSF plot (Fig. 4) shows the fluctuation in atomic residues of the protein. The peaks of the plots depict the maximum fluctuation. Alpha helix (represented by an orange background of the plot) and beta-sheet (represented by a light blue background of the plot) are the more rigid parts of the protein, as compared to the loop (represented by the white background of the plot).  $\Omega$ -loop plays an important role in the positioning of Glu166, which is involved in the hydrolytic reaction of the  $\beta$ -lactam ring present in the antibiotic substrate. Further,  $\Omega$ -loop forms the wall of the

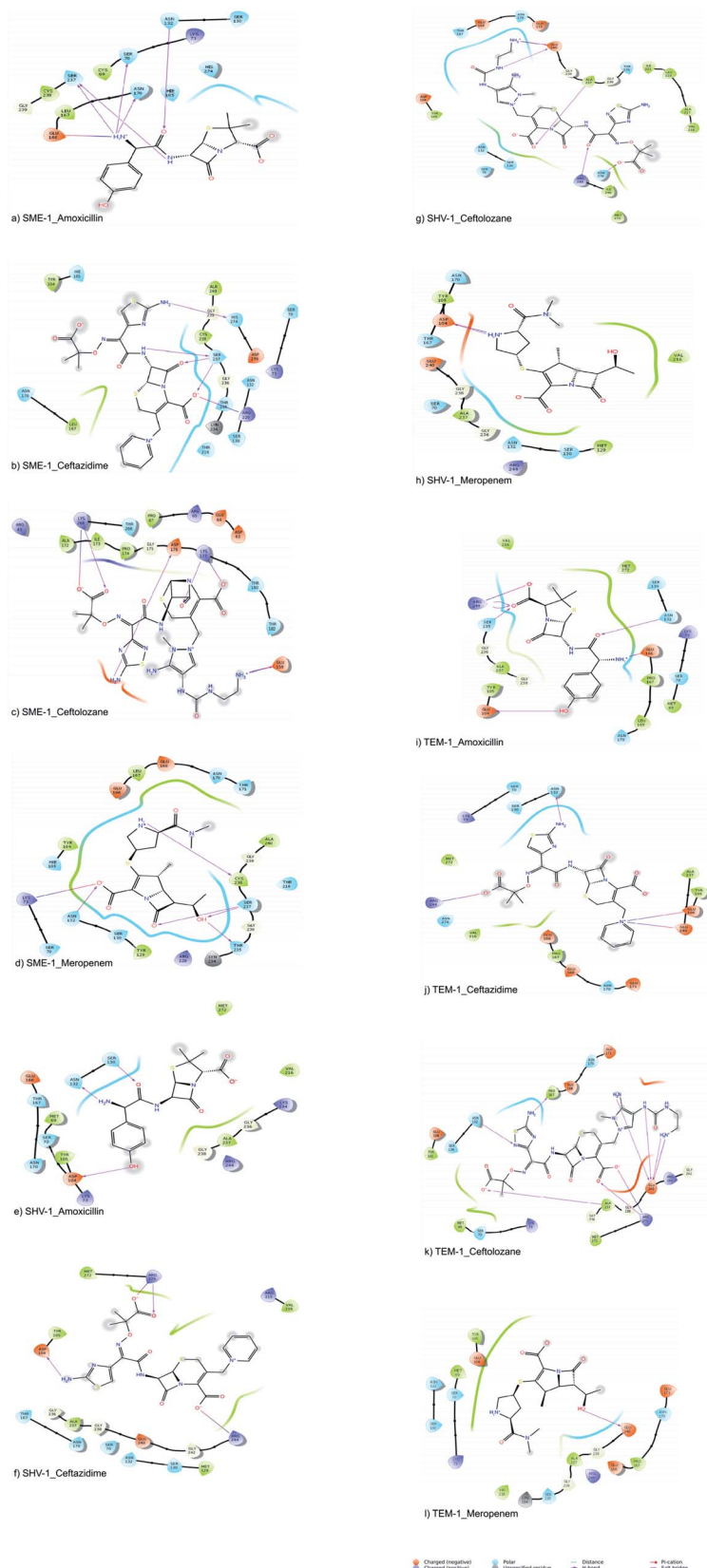


**Table 3** Class A  $\beta$ -lactamase enzymes with their docking and MMGBSA energy scores, as compared with wild-type TEM1 in complex with amoxicillin, ceftazidime, ceftazidime, and meropenem. This depicts the difference in the binding affinity of different clinically mutated class  $\beta$ -lactamase enzymes, derived from different organisms that show the difference in  $\beta$ -lactam antibiotic binding

Organism	Protein (class A $\beta$ -lactamase enzyme)-ligand ( $\beta$ -lactam antibiotics)	PDB ID of class A $\beta$ -lactamase enzyme	Glide gscore	Glide energy	emodel dg Bind	MMGBSA dg Bind	MMGBSA dg Coulomb	MMGBSA dg Covalent	MMGBSA dg Bind	MMGBSA dg Bind Solv GB	MMGBSA dg Bind vdW
<b><i>Serratiamarsenes</i></b>											
	<b>SME1</b>	<b>1DY6</b>	-4.942	-5.134	-41.488	-49.541	-34.84	-26.72	4.7	-0.93	38.14
	Amoxicilline	-5.291	-5.291	-49.394	-62.62	-37.85	-22.74	5.61	-2.06	48.93	-33.44
	Ceftazidime	-6.341	-6.342	-52.602	-81.153	-62.68	-10.32	4.29	-8.5	22	-47.12
	Ceftolozone	-4.857	-4.886	-40.394	-54.498	-41.361	-6.32	1.579	-1.577	13.069	-43.51
	<b>Meropenem</b>										-37.487
<i>Citrobactereslaki</i>		<b>3BFE</b>	-7.415	-8.181	-37.841	-49.037	-36.32	-45.35	2.04	-4.73	52.34
	Amoxicilline	-4.492	-4.492	-48.263	-65.276	-57.02	-8.64	-0.65	-2.95	21.91	-26.41
	Ceftazidime	-6.458	-6.46	-59.385	-85.323	-46.9	-21.79	6.3	-4.96	36.73	-38.39
	Ceftolozone	-4.136	-4.165	-33.83	-44.618	-23.305	-0.325	2.211	-1.981	26.494	-39.93
	<b>Meropenem</b>										-36.604
<i>Burkholderiaperseudomallei</i>		<b>3W4P</b>	-3.627	-3.82	-32.541	-46.383	-22.78	-23.36	7.14	-4.21	41.94
	Amoxicilline	-3.953	-3.953	-55.889	-73.136	-27.91	-11.72	10.12	-3.41	51.55	-26.4
	Ceftazidime	-7.981	-7.982	-67.92	-93.033	-54.3	34.84	6.73	-4.92	-20.19	-46.25
	Ceftolozone	-6.124	-6.153	-36.822	-44.807	-39.215	-24.305	3.447	-2.518	27.643	-47.07
	<b>Meropenem</b>										-31.139
<i>GHS14</i>		<b>3TSG</b>	-4.013	-4.205	-38.355	-48.642	-30.32	114.82	8.22	-0.89	-103.2
	Amoxicilline	-4.517	-4.517	-40.457	-48.753	-33.53	144.09	8.89	-2.39	-115.08	-27.71
	Ceftazidime	-6.895	-6.897	-58.641	-81.308	-69.42	7.17	6.91	-4.84	5.32	-43.83
	Ceftolozone	-3.958	-3.987	-32.504	-42.522	-13.615	55.736	2.849	-0.815	-31.539	-53.53
	<b>Meropenem</b>										-30.15
<i>Acinetobacterbaumanni</i>		<b>3V3R</b>	-5.066	-5.831	-38.753	-45.828	-38.23	-19.54	5.41	-1.54	23.16
	Amoxicilline	-5.398	-5.398	-37.045	-47.583	-37.59	37.01	0.63	-5.56	-20.3	-25.73
	Ceftazidime	-8.738	-8.739	-63.906	-96.889	-82.99	6.68	-0.45	-10.31	-9.36	-32.62
	Ceftolozone	-4.304	-4.333	-38.314	-46.366	-21.596	23.909	8.066	-0.526	-5.268	-47.13
	<b>Meropenem</b>										-35.522
<i>Acinetobacterbaumanni</i>		<b>GES11</b>	-5.066	-5.831	-38.753	-45.828	-38.23	-19.54	5.41	-1.54	23.16
	Amoxicilline	-5.398	-5.398	-37.045	-47.583	-37.59	37.01	0.63	-5.56	-20.3	-43.83
	Ceftazidime	-8.738	-8.739	-63.906	-96.889	-82.99	6.68	-0.45	-10.31	-9.36	-53.53
	Ceftolozone	-4.304	-4.333	-38.314	-46.366	-21.596	23.909	8.066	-0.526	-5.268	-30.15
	<b>Meropenem</b>										-30.15
<i>Citrobacterfreundi</i>		<b>4D2O</b>	-4.99	-5.183	-47.685	-62.932	-47.01	0.37	3.26	-1.29	14.18
	Amoxicilline	-7.391	-7.391	-60.736	-79.905	-71.68	-16.27	9.84	-2.91	21.72	-40.56
	Ceftazidime	-7.424	-7.425	-67.906	-94.476	-77.89	1.09	10.24	-9.35	7.75	-51.24
	Ceftolozone	-4.439	-4.468	-40.214	-51.792	-33.47	10.138	4.783	-1.129	8.124	-53.22
	<b>Meropenem</b>										-43.564
<i>CTXM9</i>		<b>1YIJ</b>	-5.265	-6.03	-42.948	-53.93	-34.04	-62.42	8.68	-5.09	63.49
	Amoxicilline	-4.093	-4.093	-36.929	-44.897	-33.99	84.03	0.25	-1.79	-56.75	-24.3
	Ceftazidime	-9.379	-9.38	-59.672	-75.677	-61.27	-24.97	-6.38	-8.71	20.3	-32.52
	Ceftolozone	-5.518	-5.547	-37.452	-46.731	-19.007	-8.192	6.083	-2.741	15.283	-20.677
	<b>Meropenem</b>										-32.37
<i>CTXM27</i>		<b>1YLP</b>	-4.117	-4.882	-37.016	-45.379	-41.21	-45.76	1.56	-1.18	45.43
	Amoxicilline	-5.364	-5.364	-46.69	-56.532	-40.85	13.55	5.63	-1.44	-1.09	-27.09
	Ceftazidime	-7.156	-7.158	-57.214	-69.598	-71.1	-54.77	4.4	-6.63	48.98	-40.46
	Ceftolozone	-5.029	-5.058	-33.846	-42.849	-27.498	-11.109	1.58	-2.402	22.535	-40.75
	<b>Meropenem</b>										-30.742
<i>Escherichia coli</i>											

Table 3 (Contd.)

Organism	Protein (class A $\beta$ -lactamase enzyme)-ligand ( $\beta$ -lactam antibiotics)	PDB ID of class	A $\beta$ -lactamase enzyme	Docking score	Glide gscore	Glide energy	emodel	MMGBSA dG Bind					
<i>Escherichia coli</i>													
	<b>TEM1</b>	<b>1ZG4</b>		-6.437	-7.203	-50.66	-54.842	-34.535606	-20.08852	3.132864	-4.374707	34.175854	38.996207
	Amoxicilline		-3.541	-46.618	-50.295	-33.784927	48.923797	7.830532	-1.263179	-1.263179	-24.075503	-48.803743	
	Ceftazidime		-5.845	-5.847	-53.88	-72.924	-15.725121	6.46532	7.521848	-5.716508	33.881889	-49.645526	
	Cefotolozane		-3.799	-3.828	-41.673	-54.431	-32.69	1.2	3.647	-2.021	17.335	-41.0225	
	<b>Meropenem</b>	<b>1BUE</b>		-4.582	-4.775	-38.645	-44.203	-33.75	26.13	0.89	-1.17	-11.33	-33.4
	NMCA		-3.718	-3.718	-44.239	-55.188	-22.63	43.05	-0.89	-2.32	-4.5	-40.23	
	Amoxicilline		-4.668	-4.67	-56.137	-75.439	-51.59	33	3.92	-3.04	-6.49	-54.72	
	Ceftazidime		-4.167	-4.196	-33.267	-41.508	-29.996	4.995	6.768	-1.698	4.119	-34.295	
<i>Enterobacter cloacae</i>													
	<b>TEM52</b>	<b>1HTZ</b>		-6.332	-7.097	-40.46	-47.087	-33.308	376	-11.446 065	-2.479 853	-3.685 972	30.414 074
	Amoxicilline		-5.863	-5.863	-48.459	-58.224	-35.548	678	45.387 819	1.8867	-4.815 511	-30.422 939	-35.844 801
	Ceftazidime		-7.728	-7.729	-63.368	-89.607	-43.727	577	-8.678 022	12.599 606	-7.620 953	15.554 243	-44.924 203
	Cefotolozane		-4.58	-4.609	-36.306	-48.323	-39.535	1.909	4.728	-1.71	7.148	-40.46	
	<b>Meropenem</b>												
<i>Klebsiella pneumoniae</i>													
	<b>SHV1</b>	<b>1SHV</b>		-3.501	-3.694	-36.025	-43.964	-30.387442	-41.393498	2.315058	-3.007014	51.627833	-30.99642
	Amoxicilline		-4.014	-4.014	-43.961	-49.525	-39.270824	-17.562772	8.542979	-2.90362	31.825936	-46.806289	
	Ceftazidime		-4.558	-4.559	-65.063	-81.931	-28.856741	-24.442419	10.976806	-6.497273	56.030517	-53.672098	
	Cefotolozane		-3.319	-3.348	-30.939	-38.68	-30.816	-25.064	0.772	-2.009	39.061	-33.654	
	<b>Meropenem</b>												
<i>Pseudomonas aeruginosa</i>													
	<b>FER1</b>	<b>1E25</b>		-6.151	-6.916	-46.751	-65.182	-26.33	7.98	-4.26	-1.07	-1.48	-13.23
	Amoxicilline		-4.978	-4.978	-51.766	-67.484	-27.03	-17.43	0.57	-1.04	16.12	-8.44	
	Ceftazidime		-8.214	-8.215	-58.015	-79.262	-18.68	9.03	-0.59	-0.01	-1.04	-12.67	
	Cefotolozane		-5.586	-5.615	-40.571	-57.362	-41.03	-14.776	0.931	-1.6	26.921	-41.567	
	<b>Meropenem</b>												
	<b>GHS2</b>	<b>3N19</b>		-3.645	-4.41	-32.32	-39.426	-38.16	-6.57	2.43	-6.02	14.51	-26.66
	Amoxicilline		-1.975	-1.977	-40.605	-43.059	-42.43	-5.57	13.47	-4.27	12.07	-39.81	
	Piperacillin		-2.916	-2.916	-40.856	-53.222	-30.55	-2.99	4.84	-4.77	15.53	-29.87	
	Ceftazidime		-3.966	-3.968	-49.424	-56.246	-51.69	-8.77	10.3	-11.62	18.69	-39.09	
	Cefotolozane		-3.051	-3.08	-25.021	-27.526	-22.62	-8.559	5.576	-2.225	10.384	-23.373	
	<b>Meropenem</b>												
	<b>GHS5</b>												
	Amoxicilline		-4.833	-5.598	-41.477	-52.856	-42.59	-21.55	1.89	-1.71	32.72	-31.6	
	Ceftazidime		-3.862	-3.862	-38.618	-47.176	-56.46	-18.02	0.74	-7.64	28.07	-37.81	
	Cefotolozane		-5.386	-5.387	-48.971	-73.875	-39.27	30.95	0.62	-5.32	-4.51	-39.02	
	<b>Meropenem</b>		-3.352	-3.381	-37.002	-48.355	-37.45334	-6.317 118	2.545 355	-1.538 386	13.09869	-34.729 868	
	<b>Pseudomonas aeruginosa</b>												



Legend:

Fig. 2 Shows the interaction diagram after docking between (a) SME-1\_Amoxicillin (b) SME-1\_Ceftazidime (c) SME-1\_Ceftolozane (d) SME-1\_Meropenem (e) SHV-1\_Amoxicillin (f) SHV-1\_Ceftazidime (g) SHV-1\_Ceftolozane (h) SHV-1\_Meropenem (i) TEM-1\_Amoxicillin (j) TEM-1\_Ceftazidime (k) TEM-1\_Ceftolozane (l) TEM-1\_Meropenem.



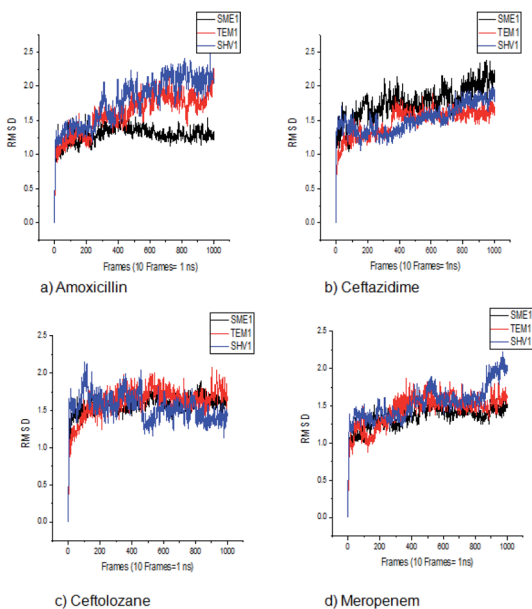


Fig. 3 The RMSD plot of clinically mutated class A  $\beta$ -lactamase enzymes (SME-1 and SHV-1) and wild class A  $\beta$ -lactamase enzyme TEM-1 in complex with (a) amoxicillin (b) ceftazidime (c) ceftolozane (d) meropenem.

active site, and hence its flexibility may indicate any structural and conformational modification in the active site. The  $\Omega$ -loop (residue 164–179) flexibility was decreased in SME-1 in complex with  $\beta$ -lactam antibiotics (amoxicillin, ceftazidime, ceftolozane, and meropenem), as compared to that with TEM-1. This is evident from the data in Table 2, Table 4, and Fig. 4.

### Interaction analysis

SME-1 and SHV-1 are naturally mutated class A  $\beta$ -lactamase and have different binding and activity towards amoxicillin, ceftazidime, ceftolozane, and meropenem, per the molecular docking and molecular dynamic simulations results. This analysis can help us to gain insight into the altered active site residue interactions. According to the molecular docking and molecular dynamics simulation studies, SME-1 has a good binding affinity throughout the simulation of 100 ns with meropenem, as compared to TEM-1 and SHV-1 (Table 2 and Fig. 3).

It was observed that Tyr104 (in SME-1) has an increased interaction fraction with amoxicillin and meropenem (Fig. 5a and d), as compared to Asp104 (in SHV-1) interaction fraction and Glu104 (in TEM-1) interaction fraction with all the  $\beta$ -lactam antibiotics considered in the study, including meropenem (Fig. 5).

SME-1, Ser237, and Cys238 show significant interaction with meropenem, whereas Ala237 and Gly238 (in SHV-1 and TEM-1) do not interact much with meropenem (Fig. 5d, h, and l).

Tyr104 in SME-1 forms a significant and constant interaction for 100 ns, which is absent in the case of SHV-1 and TEM-1 in complex with meropenem (Fig. 6d, h, and l). His105 shows slight interaction with SME-1 after 25 ns, with meropenem

(Fig. 6d) but no interaction with TEM-1 after 25 ns, or meropenem (Fig. 6l).

### Principal component analysis

Principal component analysis (PCA) was performed to understand the correlation between the secondary structure fragments of the complex along with the contribution of its residues. This could help in gaining insights into the protein complex dynamics by analyzing the coefficients of the principal components.<sup>14</sup> Protein biological function is governed by protein conformations and their dynamics. A functional protein demonstrates flexibility and rigidity of its constituent residues to a different extent. Protein-ligand stability means that there is a tighter interaction between the active site residues of the protein and the ligand. Further, it could also mean that this complex becomes stable and its motion is restricted to some extent. Thus, the conformation of the biologically active proteins results in activity. Hence, for understanding the collective motion of the protein-ligand complex present in the conformational space for the molecular dynamics simulations, the dimension reduction method or the essential dynamic calculations is an appropriate analysis for projecting principal component 1 (PC1) and principal component 2 (PC2). This calculation was performed by diagonalizing the covariance matrix of the eigenvectors, for understanding the subspaces in which most of the protein dynamics occur.<sup>15</sup> The PCA plot of SME-1, SHV-1, and TEM-1 in complex with amoxicillin, ceftazidime, ceftolozane, and meropenem shows that SME-1 is more stable, compared with SHV-1 and TEM-1 with meropenem and amoxicillin (Fig. 7). This observation leads to the conclusion that mutations in SME-1, as compared to TEM-1 and SHV-1, result in better binding with ligands such as amoxicillin and meropenem. RMSD plot also shows that SME-1 has a better binding with amoxicillin and meropenem, as compared to those in TEM-1 and SHV-1. This means that the mutations that occur uniquely in SME-1, as compared to in TEM-1 and SHV-1 could be responsible for altering the binding properties of SME-1 with amoxicillin and meropenem.

### Residue interaction analysis

Ser70, Lys73, Ser130, Asn132, Glu166, and Asn170 are residues that directly participate in the catalytic hydrolysis of  $\beta$ -lactam antibiotics. However, several other important residues are uniquely mutated in SME-1, which could play an important role in altering the structure of the enzyme and thus are responsible for carbapenemase activity. This could be due to the local structural modification, which results from the altered interactions and hydrogen bonding patterns with  $\beta$ -lactam antibiotics. Fig. 8 shows the modification in the interaction pattern in SME-1, as compared to that in TEM-1. Fig. 8a shows the interaction between mutated residues with their closest associated residues in SME-1, whereas Fig. 8b shows the same for the TEM-1 enzyme. It can be observed that residues 69, 104, 105, 237, and 238 are mutated in SME-1, as compared to the wild-type TEM-1 enzyme. These mutated residues are closely connected with Ser70, Lys73, Ser130, Asn132, Glu166, and Asn170 residues,



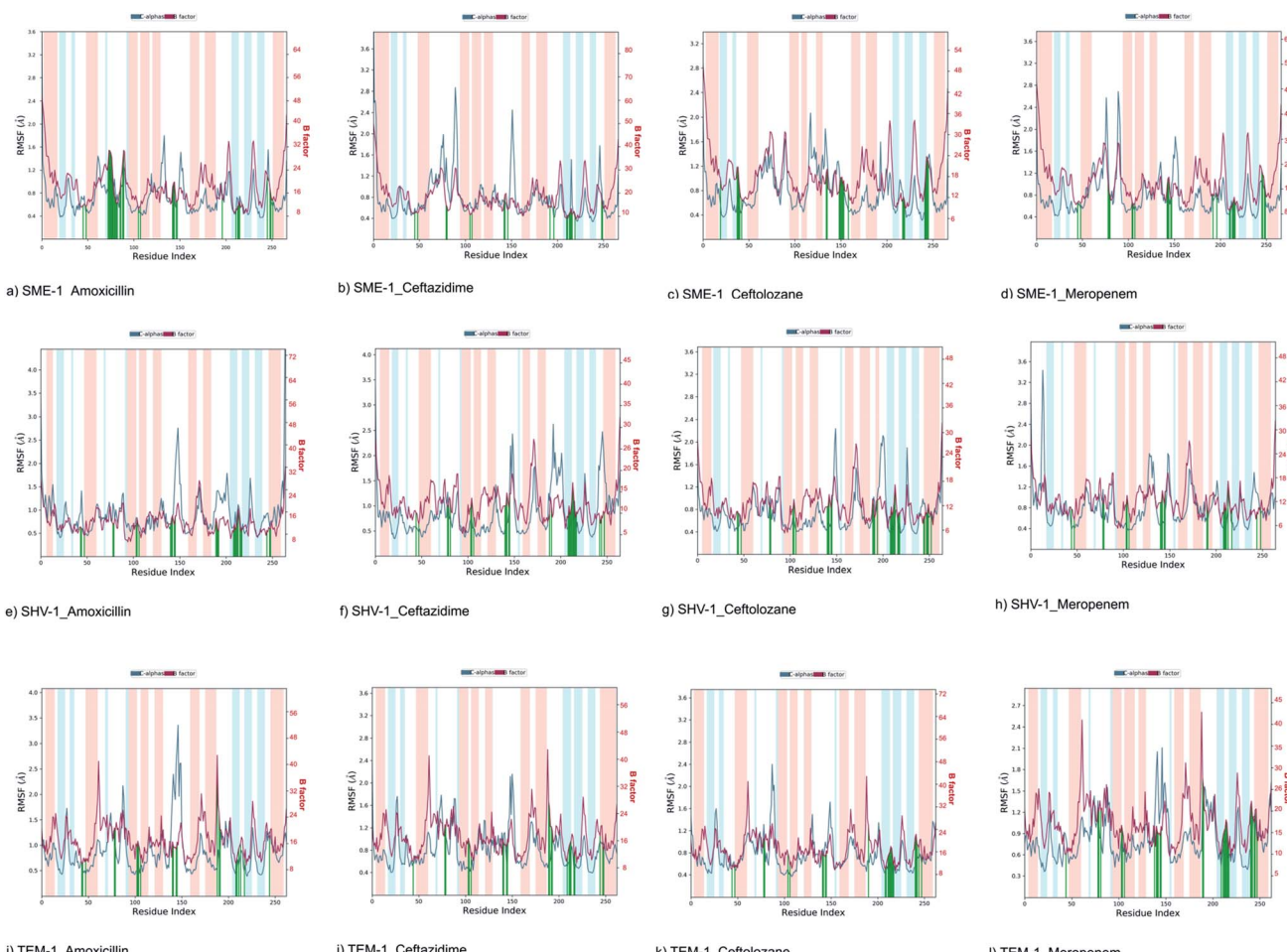


Fig. 4 Shows the RMSF plot and B factor plot of (a) SME-1\_Amoxicillin (b) SME-1\_Ceftazidime (c) SME-1\_Cefotolozane (d) SME-1\_Meropenem (e) SHV-1\_Amoxicillin (f) SHV-1\_Ceftazidime (g) SHV-1\_Cefotolozane (h) SHV-1\_Meropenem (i) TEM-1\_Amoxicillin (j) TEM-1\_Ceftazidime (k) TEM-1\_Cefotolozane (l) TEM-1\_Meropenem complex. Alpha helix (represented by the orange background of the plot), and beta-sheet (represented by the light blue background of the plot) are the loop regions (represented by the white background of the plot). Green lines show the residues of protein that interact with the ligand.

Table 4 RMSF values calculated for clinically mutated class A  $\beta$ -lactamases (SME-1 and SHV-1) and wild class A  $\beta$ -lactamase (TEM-1) in complex with meropenem

Residue	SME-1	SHV-1	TEM-1
Ser70	0.755	0.378	0.43
Lys73	0.457	0.348	0.39
Ser130	0.649	0.357	0.427
Asp131	0.544	0.334	0.362
Asn132	0.572	0.32	0.379
Arg164	0.75	0.398	0.493
Trp165	1.019	0.4	0.523
Glu166	0.859	0.406	0.517
Glu168	0.794	0.476	0.561
Leu169	0.686	0.388	0.476
Asn170	0.756	0.438	0.469
Ala172	0.859	0.69	0.57
Pro174	2.795	2.654	1.295
Asp176	2.085	1.581	0.924
Arg178	1.077	0.629	0.611
Asp179	0.642	0.432	0.461

which participate in the hydrolytic reactions of  $\beta$ -lactam antibiotics.

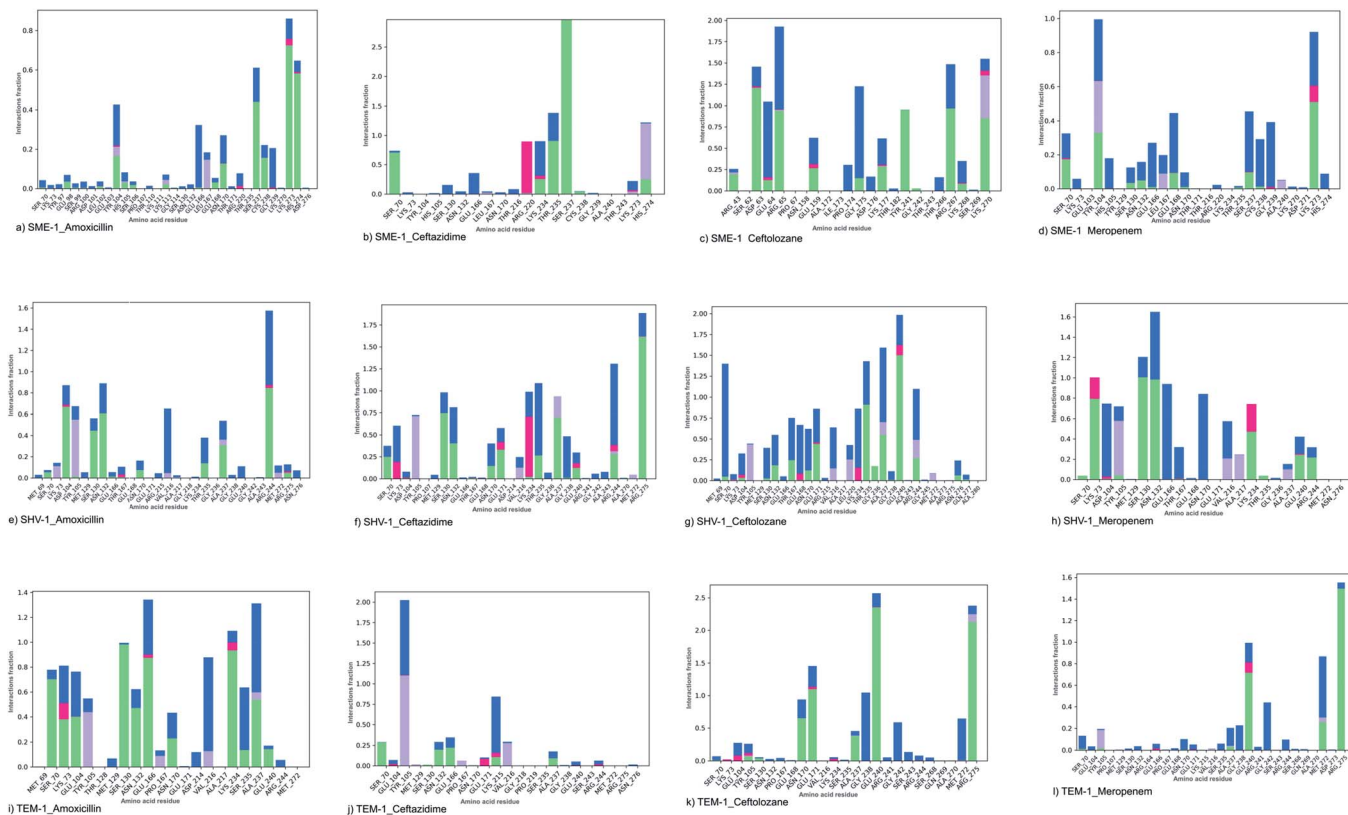
#### MMGBSA calculations of the MD trajectory

To explore the effect of clinical mutations in SME-1 compared to TEM-1 on binding with meropenem, MMGBSA of MD trajectory of class A  $\beta$ -lactamase enzymes (SME-1 and TEM-1) with  $\beta$ -lactam antibiotics were calculated. The average  $dG_{bind}$  is lower ( $-75.04\ 087\ 792\ \text{kcal mol}^{-1}$  and  $-59.0031\ \text{kcal mol}^{-1}$ ) for SME-1, as compared with TEM-1 ( $-68.8181\ \text{kcal mol}^{-1}$  and  $-56.7565\ \text{kcal mol}^{-1}$ ) in the complex with amoxicillin and meropenem, respectively. This shows that SME-1 is more stable, as compared to SHV-1 and TEM-1 with meropenem and amoxicillin (Table 5).

#### Per residue binding free energy decomposition analysis

The decomposition of the binding energy into 5 key mutated residues is shown in this analysis. These mutated residues are closely connected with residues involved in the hydrolytic





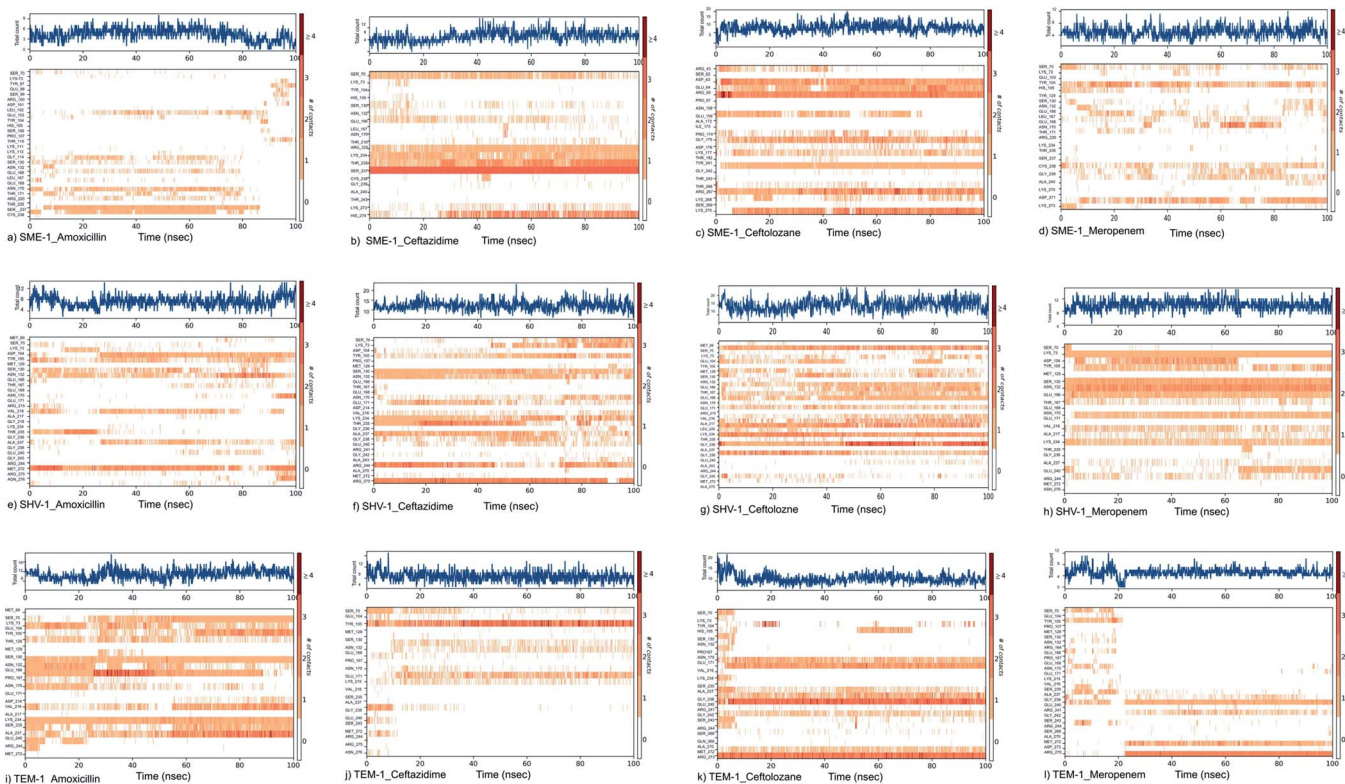


Fig. 6 Shows the timeline representation of interaction and contact between (a) SME-1\_Amoxicillin (b) SME-1\_Ceftazidime (c) SME-1\_Ceftolozane (d) SME-1\_Meropenem (e) SHV-1\_Amoxicillin (f) SHV-1\_Ceftazidime (g) SHV-1\_Ceftolozane (h) SHV-1\_Meropenem (i) TEM-1\_Amoxicillin (j) TEM-1\_Ceftazidime (k) TEM-1\_Ceftolozane (l) TEM-1\_Meropenem.

study with respect to wild type TEM-1. Further, SME-1 in the complex with meropenem shows the maximum deviation in conserved residues like Ser70, Lys73, Ser130, Asn132, Glu166, and Asn170 compared to naturally mutated SHV-1 and wild-type TEM-1 class A  $\beta$ -lactamase enzymes (Table 4 and Fig. 10).

Residues 69, 70, 73, 104, 105, 166, 170, 237, and 238 (mutated residues and residues, which are involved in the hydrolytic reaction with  $\beta$ -lactam antibiotics) showed a significant deviation in naturally mutated class A  $\beta$ -lactamase enzyme SME-1, as compared to naturally mutated class A  $\beta$ -lactamase enzyme SHV-1 and wild class A  $\beta$ -lactamase enzyme TEM-1.  $\Omega$ -loop forms the wall of the active site and is the most flexible element of the active site. Hence, its structure alteration depicts an altered active site structure of SME-1 enzyme, as compared to TEM-1 in complex with meropenem (Fig. 10b).

Alterations in the H-bonding pattern can be observed in Tyr104 of SME-1, as compared to those in Asp104 of SHV-1 and Glu104 of TEM-1 (Fig. 2d, h, and l). Tyr104 has an increased interaction fraction in SME-1, as compared with that in Asp104 in SHV-1 and Glu104 in TEM-1 with meropenem (Fig. 5d, h and l). Tyr104 is directly linked with Leu167 residue, which is further linked to Asn170 and Asn132 residues that are important catalytic residues in SME-1 (Fig. 8a). Whereas, Glu104 is linked with the Pro167 residue, which is further linked with only Asn170 in wild-type TEM-1 enzyme (Fig. 8b). Further, it can be observed that Tyr104 has a lower dG binding in SME-1, as compared to

that in Glu104 in TEM-1 in complex with meropenem (Fig. 9). As 104 residue is closely connected with residues, which are involved in the hydrolytic reaction with  $\beta$ -lactam antibiotics such as Asn130 and Asn170, mutation results in the displacement of Tyr104 in SME-1 with respect to Asp104 in SHV-1 and Glu104 in TEM-1 with meropenem, as shown in the 50 ns time frame of the MD simulation (Fig. 10). So, it can be concluded that Glu104Tyr mutation results in some structural modifications in the active site of SME-1 and as it is linked to residues, which are involved in the hydrolytic reaction with  $\beta$ -lactam antibiotics such as Asn170 (part of  $\Omega$ -loop) and Asn132 (part of SDN loop), as compared to wild type TEM-1.

His105 of SME-1 forms a polar interaction with meropenem, whereas Tyr105 of SHV-1 and TEM-1 forms a hydrophobic interaction with meropenem (Fig. 2d, h, and l). His105 in SME-1 forms a link with Ser130, Asn132 and Tyr129 (Fig. 8a). Tyr105 in TEM-1 forms a link with Ser130 and Asn132 (Fig. 8b). Both the residues are of catalytic importance and form part of the SDN loop. His105 in SME-1 has a lower dG binding value, as compared to Tyr105 in TEM-1 (Fig. 9). His105 in SME-1 shows a structural deviation, as compared to Tyr105 of SHV-1 and TEM-1 (Fig. 10), and is linked to residues, which are involved in the hydrolytic reaction with  $\beta$ -lactam antibiotics and loops like Ser130, Asn132, and SDN loop, respectively. This observation was made in a complex with meropenem at 50 ns of MD simulation (stable state). So, it can be concluded that the



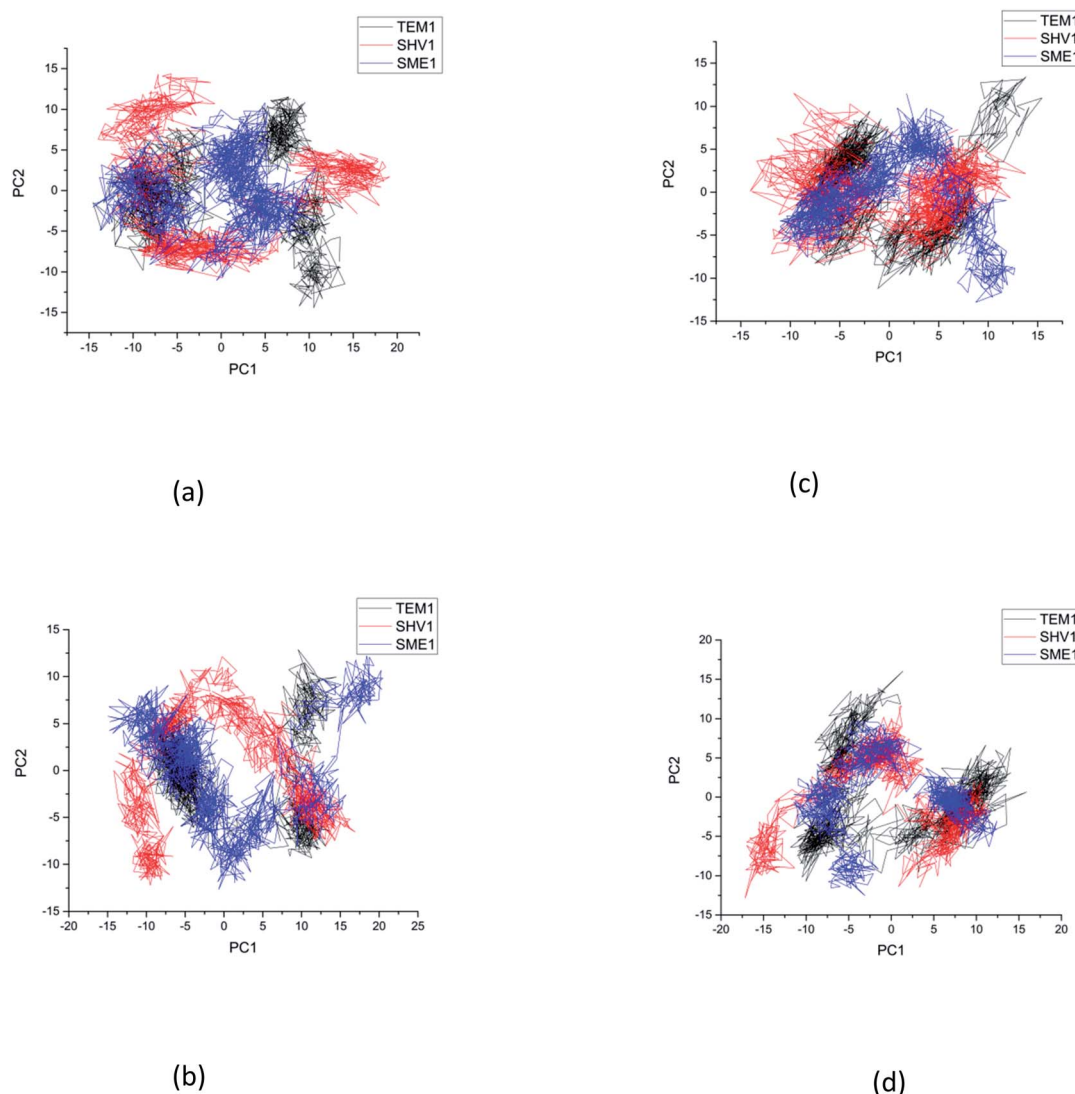


Fig. 7 The principal component analysis of clinically mutated class A  $\beta$ -lactamase enzymes (SME-1 and SHV-1) and wild class A  $\beta$ -lactamase enzyme TEM-1 with (a) amoxicillin (b) ceftazidime (c) ceftolozane (d) meropenem.

Tyr105His mutation results in structural modifications that could alter the binding of ligands such as meropenem.

Similarly, Ala237Ser and Gly238Cys mutations in SME-1 result in H-bond formation in SME-1, which is absent in SHV-1 and TEM-1 with meropenem. A previous study demonstrated that the formation of a disulphide bond in class A  $\beta$ -lactamase enzymes at Cys69 and Cys238 is important for the catalytic activity against most of the  $\beta$ -lactam antibiotics including carbapenems.<sup>16</sup> Ser237 and Cys238 are directly linked with Cys69 in SME-1 (Fig. 8a). These interactions are altered in TEM-1, as the Met69 residue is connected with Ala237 and Ser234, which is further connected with Gly238 (Fig. 8b).

Active site structure is directly related to the function and activity of an enzyme.  $\Omega$ -Loop structure alteration in the case of SME1 (compared to wild TEM1 and clinically mutated SHV1) shows its altered active site at 50 ns, which is a stable state of molecular dynamic simulation. It can be observed from the

residue decomposition analysis that the dGbind value is different in the case of all the key mutated residues such as 69, 104, 105, 237, and 238 in SME1, as compared with that in TEM1. Further, it can be observed from Fig. 10 that the mutated (Met69Cys, Glu104Tyr, Tyr105His, Ala237Ser, and Gly238Cys) and active site catalytically important residues (Ser70, Lys73, Ser130, Asn132, Glu166, and Asn170) are relocated in SME1, as compared with TEM1 and SHV1. These observations give evidence of the structural analysis, which is correlated with the enzymatic activity with residues.

As residues 69, 104, 105, 237, and 238 are closely connected to residues, which are involved in the hydrolytic reaction with  $\beta$ -lactam, antibiotics such as Ser70, Lys73, Ser130, Asn132, Glu166, and Asn170, and their mutation results in altered interactions with residues, which are involved in the hydrolytic reaction with  $\beta$ -lactam antibiotics, which are involved in the catalytic reaction with meropenem as well as with meropenem,



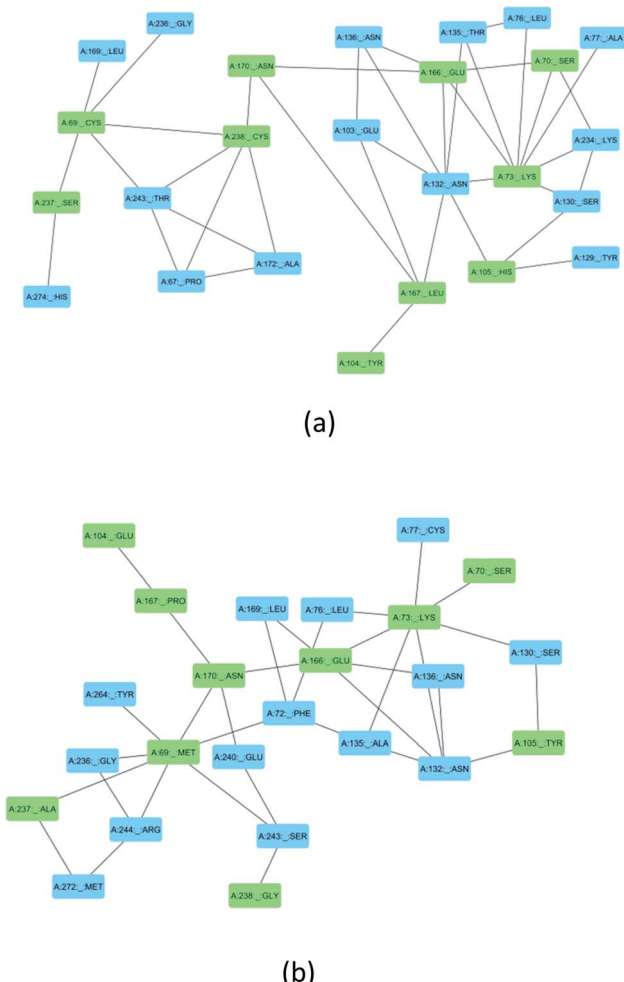


**Fig. 8** (a) Shows the residue interaction network of the SME-1 enzyme (b) Shows the residue interaction network of TEM-1 enzyme. The green colour shows mutated residues along with the residues of catalytic importance and the blue colour shows its neighbouring residues that directly interact with mutated residues

which is a carbapenem. These structural modifications could result in active site plasticity and altered binding with carbapenems in SME-1 class A  $\beta$ -lactamase enzymes. Hence, it could be concluded that Met69Cys, Glu104Tyr, Tyr105His, Ala237Ser, and Gly238Cys mutations occur in SME-1 and result in altered

interactions with residues, which are involved in the hydrolytic reaction with  $\beta$ -lactam antibiotics.

## Materials and methods

## Kinetics analysis

The catalytic efficiency ( $K_{\text{cat}}/k_m$ ) was derived based on a literature survey for the kinetic analysis of SME-1 with other naturally mutated and wild-type classes A  $\beta$ -lactamase enzymes.

## Sequence analysis

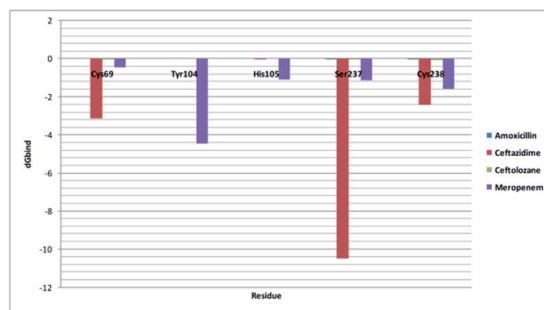
FASTA sequences of 14 naturally mutated class A  $\beta$ -lactamase enzymes TEM-52 (PDB ID: 1HTZ), SHV-1 (PDB ID: 1SHV), SME-1 (PDB ID: 1DY6), NMC-A (PDB ID: 1BUE), SED-1 (PDB ID: 3BFE), CTXM-9 (PDB ID: 1YJL), CTXM-27 (PDB ID: 1YLP), PENI (PDB ID: 3W4P), GES-2 (PDB ID: 3NI9), GES-11 (PDB ID: 3V3R), GES5 (PDB ID: 4GNU), PER-1 (PDB ID: 1E25) and PER-2 (PDB ID: 4D2O) and wild type class A  $\beta$ -lactamase enzymes (TEM-1) were derived from RCSB-PDB database. These sequences were compared using the multiple sequence alignment tool Multalign.<sup>17</sup> Furthermore, a phylogenetic tree was formed using Clustal W.

## Structure analysis

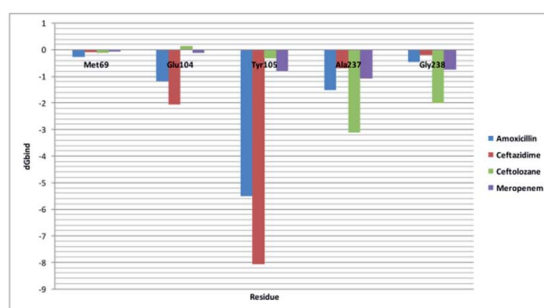
The structure of 14 naturally mutated class A  $\beta$ -lactamase enzymes TEM-52 (PDB ID: 1HTZ), SHV-1 (PDB ID: 1SHV), SME-1 (PDB ID: 1DY6), NMC-A (PDB ID: 1BUE), SED-1 (PDB ID: 3BFE), CTXM-9 (PDB ID: 1YLJ), CTXM-27 (PDB ID: 1YLP), PENI (PDB ID: 3W4P), GES-2 (PDB ID: 3NI9), GES-11 (PDB ID: 3V3R), GES5 (PDB ID: 4GNU), PER-1 (PDB ID: 1E25) and PER-2 (PDB ID: 4D2O) were derived in the PDB format from RCSB-PDB database. PyMOL Molecular Graphics System, Version 2.0 Schrödinger, LLC (academic version) was used to visualize and compare enzyme structure of naturally mutated and wild-type class A  $\beta$ -lactamase enzymes. Furthermore, RMSD values of all the naturally mutated class A  $\beta$ -lactamase enzymes were calculated, as compared to wild-type TEM-1 using the PyMOL Molecular Graphics System, Version 2.0 Schrödinger, LLC (academic version). Structures of SME-1, SHV-1, and TEM-1 in complex with meropenem at 50 ns (stable state during MD simulation), were aligned to each other for comparing their structural features.

**Table 5** Shows the MMGBSA calculations of the SME-1 and TEM-1 MD trajectory in the complex with meropenem.

Protein (Class A $\beta$ -lactamase)	Ligand ( $\beta$ -lactam antibiotics)	MMGBSA dG Bind	MMGBSA dG Bind Coulomb	MMGBSA dG Bind Covalent	MMGBSA dG Bind Hbond	MMGBSA dG Bind Solv GB	MMGBSA dG Bind vdW
SME-1	Amoxicillin	-75.04 087 792	-16.22 674 604	5.636 274 192	-9.607 015 983	21.21 115 165	-48.61 465 048
	Ceftazidime	-83.5186	-75.4778	3.86303	-5.550 947 299	65.95 994 743	-49.43 714 579
	Ceftolozane	-70.3896	14.8433	1.83726	-7.30828	-1.57884	-50.367
	Meropenem	-59.0031	-35.0996	5.099636	-0.66614	50.0101	-40.6197
TEM-1	Amoxicillin	-68.8181	-80.0014	12.93065	-9.30847	68.84899	-39.8453
	Ceftazidime	-84.4038	-37.7148	0.816 403	-1.64518	40.76461	-50.9933
	Ceftolozane	-81.014	-68.1355	13.38447	-12.4592	62.71666	-52.3695
	Meropenem	-56.7565	-19.4327	2.120 725	-0.34663	33.59121	-43.3942



(a)

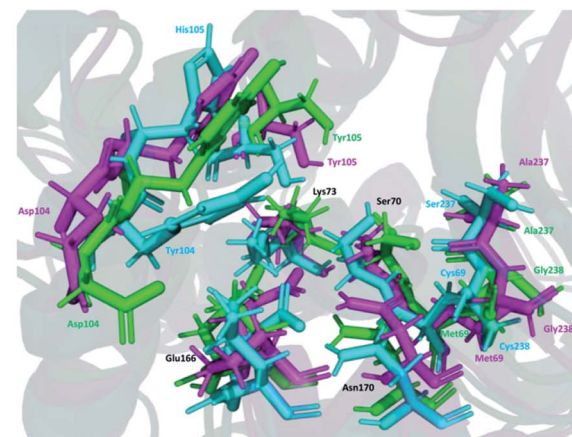


(b)

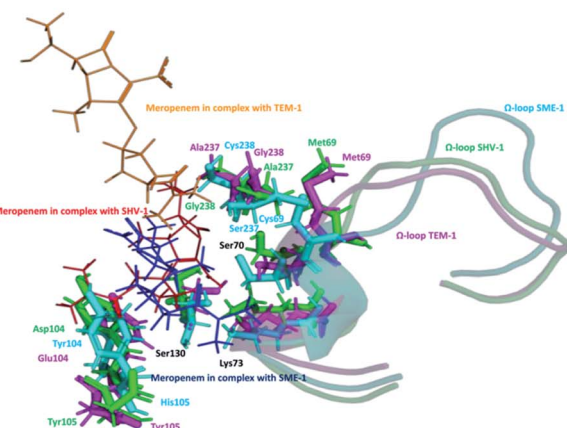
Fig. 9 (a) Shows the residue decomposition analysis for (a) clinically mutated class A  $\beta$ -lactamase enzyme SME-1 and (b) wild class A  $\beta$ -lactamase enzyme TEM-1.

### Molecular docking and MMGBSA

Protein preparation wizard suite v10.2, Schrodinger, LLC, New York, NY, 2015, was used for the protein preparation of 14 naturally mutated class A  $\beta$ -lactamase enzymes and wild-type TEM-1. Default parameters were used for scraping off steric clashes, non-essential water molecules, and hetero-atoms.<sup>18</sup> The dimensions grid box created around the active site of the target receptor were kept as inner box:  $X = 20$ ,  $Y = 20$ ,  $Z = 20$ , outer box:  $X = 20$ ,  $Y = 20$ ,  $Z = 20$  and was centered around active site residues 70, 73, 130, 132, 166, 170 and 234 using Glide v6.6, Schrodinger, LLC, New York, 2015 module.<sup>19</sup> Ligand processing was performed using Ligprep along with the Epik module and expansion of protonation and tautomeric states (7.0 + 2.0 Ph units). Five stereoisomers of low energy conformer were generated for each ligand, out of which a single three-dimensional structure (lowest energy conformation) with accurate chirality was selected for further investigation. Molecular docking of 14 naturally mutated  $\beta$ -lactamase enzymes, as well as a wild-type class A  $\beta$ -lactamase TEM-1, with amoxicillin (PubChemID: 33 613), ceftazidime (PubChemID:



(a)



(b)

Fig. 10 (a) Shows residues that are involved in the hydrolytic reaction with  $\beta$ -lactam antibiotics and are conserved (black), mutated in SME-1 (cyan), SHV-1 (green) and TEM-1 (magenta), at 50 ns (stable state of MD simulation) (b) Shows modifications in  $\Omega$ -loop structure at 50 ns (stable state of MD simulation).

5 481 173), ceftolozane (PubChemID: 56 843 746) and Meropenem (PubChemID: 441 130) using GLIDE v6.7 (Schrodinger, LLC, New York, 2015). Amoxicillin is penicillin, ceftazidime and ceftolozane are cephalosporins, and meropenem is a carbapenem.

Molecular mechanics/generalized Born surface area (MM-GBSA) of the docked protein-ligand complex was performed using Prime, Schrodinger, LLC, New York, NY, 2019–2, to evaluate the binding affinity between the enzyme and the ligand.



## Molecular dynamic simulation

Molecular dynamic (MD) simulation was executed using Desmond, incorporated in the Schrodinger suite. The OPLS 2005 force field was used for SME-1, SHV-1, and wild-type class A  $\beta$ -lactamase TEM-1. The TIP3P water model was enclosed in an orthorhombic box ( $a = 10 \text{ \AA}$ ,  $b = 10 \text{ \AA}$ ,  $c = 10 \text{ \AA}$ ) along with periodic boundary conditions. A salt concentration of  $0.15 \text{ mol L}^{-1}$  was used for charge neutralization using cation ( $\text{Na}^+$ ) or anion ( $\text{Cl}^-$ ). Energy minimization was performed using the steepest descent method with a convergence threshold of  $1.0 \text{ kcal mol}^{-1} \text{ \AA}^{-1}$ . The system's minimization and relaxation were performed using an NPT ensemble, and a  $300 \text{ K}$  temperature was maintained along with  $1.013 \text{ bar}$  pressure. MD simulation was performed for  $100 \text{ ns}$ . MD trajectory analysis was carried out via RMSD, RMSF, and hydrogen bond analysis.<sup>20</sup>

## MMGBSA of the MD trajectory

MMGBSA calculations of all protein-ligand complex MD trajectories were performed using a prime package of Schrödinger LLC. MMGBSA can be mathematically defined as follows:

$$G = E_{\text{bnd}} (\text{BONDED ENERGY}) + E_{\text{ele}} (\text{ELECTROSTATIC ENERGY}) + E_{\text{vdw}} (\text{VAN DER WAALS ENERGY}) + G_{\text{solv}} (\text{NON-POLAR SOLVATION ENERGY}) + G_{\text{npr}} (\text{SOLVENT ACCESSIBLE SURFACE AREA ENERGY}) - TS^{21}$$

## Principle component analysis

Principle component analysis (PCA) of molecular dynamics simulation helps in understanding the essential dynamics of the protein complex. Desmond simulation package of Schrödinger LLC was used for finding the essential dynamics of the 12 complex (including SME-1, SHV-1, and TEM-1 protein in complex with amoxicillin, ceftazidime, ceftolozane, and meropenem).

## Residue interaction analysis (RIN)

RIN demonstrates inter-residue interactions with the help of network formations. This method gives insights into the effect of mutation on drug resistance by showing how the interactions are altered in the case of mutated residues.<sup>22</sup> Protein (SME-1 and TEM-1) residue interaction networks were downloaded from the RING web server.<sup>23</sup> RIN analysis was performed using Cytoscape.<sup>24</sup>

## Per residue binding free energy decomposition analysis

Binding free energy calculation gives insights into the energetic contribution of the protein, binding to a ligand. This helps in understanding the specificity and sensitivity of protein-ligand interactions. This was calculated using a prime package of Schrödinger LLC. The decomposition of binding energy per residue helps in knowing the energy of different residues, which

could be important for altering the binding pattern of the protein-ligand complex.<sup>25</sup>

## Conclusions

SME-1 is a carbapenemase, which belongs to class A  $\beta$ -lactamase enzymes. Multiple sequence and structure alignment shows the presence of some unique mutations, which results in the altered binding of SME-1, as compared to other naturally mutated class A  $\beta$ -lactamase enzymes and wild-type TEM-1. SME-1 has altered binding with  $\beta$ -lactam antibiotics as evident from the molecular docking, molecular dynamic simulation, PCA, and MMGBSA analysis of the MD trajectory of SME-1, SHV-1, and TEM-1 class A  $\beta$ -lactamase enzymes in complex with  $\beta$ -lactam antibiotics. Active site alterations occur in SME-1, which is evident from the altered  $\Omega$ -loop structure and relocation of residues such as Ser70, which are involved in the hydrolytic reaction with  $\beta$ -lactam antibiotics. Molecular docking and molecular dynamic simulation interaction analysis showed that 69, 104, 105, 237, and 238 residues are mutated and show altered interaction with meropenem. Furthermore, these residues are closely connected with residues Ser70, Lys73, Ser130, Asn132, Glu166, and Asn170, which are involved in the hydrolytic reaction with  $\beta$ -lactam antibiotics including meropenem. Based on the altered interactions of 69, 104, 105, 237, and 238 residues with meropenem in SME-1, as compared with TEM-1 and its close connections with residues involved in the hydrolytic reaction, it can be concluded that Met69Cys, Glu104Tyr, Tyr105His, Ala237Ser, and Gly238Cys mutations result in structural and binding alterations with meropenem, leading to carbapenemase activity of the SME-1 class A  $\beta$ -lactamase enzyme.

## Conflicts of interest

There are no conflicts to declare.

## Acknowledgements

The authors are thankful to IIIT, Allahabad, for providing all infrastructure and facilities required for the completion of this work. Vidhu Agarwal is also thankful to Dr Robin Anderson for fruitful discussions.

## References

- 1 D. Hammoudi Halat and C. Ayoub Moubareck, *Antibiotics*, 2020, **9**, 186.
- 2 M. Biagi, A. Shajee, A. Vialichka, M. Jurkovic, X. Tan and E. Wenzler, *Antimicrob. Agents Chemother.*, 2020, **64**, 4.
- 3 A. Khanna, *JCDR*, 2013, **7**, 2.
- 4 D. S. Teklu, A. A. Negeri, M. H. Legese, T. L. Bedada, H. K. Woldemariam and K. D. Tullu, *Antimicrobial Resistance and Infection Control*, 2019, **8**, 39.
- 5 W. Sougakoff, G. L'Hermite, L. Pernot, T. Naas, V. Guillet, P. Nordmann, V. Jarlier and J. Delettre, *Acta Crystallogr., Sect. D: Biol. Crystallogr.*, 2002, **58**, 267–274.



6 W. Sougakoff, T. Naas, P. Nordmann, E. Collatz and V. Jarlier, *Biochim. Biophys. Acta, Protein Struct. Mol. Enzymol.*, 1999, **1433**, 153–158.

7 F. K. Majiduddin and T. Palzkill, *Antimicrob. Agents Chemother.*, 2003, **47**, 1062–1067.

8 F. K. Majiduddin and T. Palzkill, *Antimicrob. Agents Chemother.*, 2005, **49**, 3421–3427.

9 A. Amadei, A. B. M. Linssen, B. L. de Groot, D. M. F. van Aalten and H. J. C. Berendsen, *J. Biomol. Struct. Dyn.*, 1996, **13**, 615–625.

10 E. Laine, I. Chauvot de Beauchêne, D. Perahia, C. Auclair and L. Tchertanov, *PLoS Comput. Biol.*, 2011, **7**, e1002068.

11 T. Naas, L. Dortet and B. I. Iorga, *Curr. Drug Ther.*, 2016, **17**, 1006–1028.

12 M. L. Winkler and R. A. Bonomo, *Mol. Biol. Evol.*, 2016, **33**, 429–441.

13 A. Egorov, M. Rubtsova, V. Grigorenko, I. Uporov and A. Veselovsky, *Biomolecules*, 2019, **9**, 854.

14 C. C. David and D. J. Jacobs, in *Protein Dynamics*, ed. D. R. Livesay, Humana Press, Totowa, NJ, 2014, vol. 1084, pp. 193–226.

15 I. Daidone and A. Amadei, *Wiley Interdisciplinary Reviews: Computational Molecular Science*, 2012, **2**, 762–770.

16 C. A. Smith, Z. Nosseni, M. Toth, N. K. Stewart, H. Frase and S. B. Vakulenko, *J. Biol. Chem.*, 2016, **291**, 22196–22206.

17 F. Corpet, *Nucleic Acids Res.*, 1988, **16**, 10881–10890.

18 G. Madhavi Sastry, M. Adzhigirey, T. Day, R. Annabhimoju and W. Sherman, *J. Comput.-Aided Mol. Des.*, 2013, **27**, 221–234.

19 T. A. Halgren, R. B. Murphy, R. A. Friesner, H. S. Beard, L. L. Frye, W. T. Pollard and J. L. Banks, *J. Med. Chem.*, 2004, **47**, 1750–1759.

20 S. Gupta, V. Singh, P. K. Varadwaj, N. Chakravartty, A. V. S. K. M. Katta, S. P. Lekkala, G. Thomas, S. Narasimhan, A. R. Reddy and V. B. Reddy Lachagari, *J. Biomol. Struct. Dyn.*, 2020, 1–20.

21 P. Mikulskis, S. Genheden and U. Ryde, *J. Mol. Model.*, 2014, **20**, 2273.

22 Q. Zhang, X. An, H. Liu, S. Wang, T. Xiao and H. Liu, *Front. Chem.*, 2019, **7**, 819.

23 D. Piovesan, G. Minervini and S. C. E. Tosatto, *Nucleic Acids Res.*, 2016, **44**, W367–W374.

24 D. Otasek, J. H. Morris, J. Bouças, A. R. Pico and B. Demchak, *Genome Biol.*, 2019, **20**, 185.

25 M. K. Teli, S. Kumar, D. K. Yadav and M. Kim, *J. Cell. Biochem.*, 2021, **122**, 1098–1112.

